INSTRUMENTATION AND MEASUREMENT OF SECONDARY ELECTRON EMISSION FOR SPACECRAFT CHARGING

Neal Nickles
Physics Department, Utah State University, Logan.

Abstract

Secondary electron emission is an important physical mechanism in the problem of spacecraft charging. The NASA Space Environments and Effects branch is currently revising NASA's strategy for mitigating damage due to spacecraft charging. In an effort to substantially improve the modeling of spacecraft charging, measurements of secondary electron emission parameters are being made. The design of the apparatus needed to measure these parameters is discussed in detail. Various measurement techniques are explained and conclusions are drawn about the suitability of the final design.

Spacecraft Charging

Spacecraft in earth orbits are subjected to a harsh environment. In addition to man-made and meteor debris, large temperature extremes, and high vacuum; spacecraft travel at high velocity through the earth's plasma, which is a charged particle "soup" consisting of electrons and ions [*James, 1994*]. The spacecraft's plasma environment is characterized by electron and ion densities, as well as their distribution in energy. During heighten solar activity, changes in the earth's magnetosphere can result in extremely high energy charged particles impacting the spacecraft [*Vaughan, 1996*]. The ambient plasma and these high energy fluxes of charged particles constitute currents to the spacecraft, which results in the spacecraft accumulating charge.

In response to these currents from the plasma, the spacecraft surfaces charge to a potential that is sufficient to stop the currents and reach equilibrium. The eventual potential(s) that is reached partly depends on the characteristics of the spacecraft's plasma environment. During geomagnetic storm activity, satellites in geosynchronous orbit (GEO) have reached kilovolt levels of charging [*Whipple, 1981;Garret, 1981; Hastings, 1996*]. Even a large vehicle potential, between the spacecraft chassis ground and the neutral plasma, is not typically dangerous to spacecraft; although measurements of charged particles are confounded by these vehicle potentials.

Damage can occur when different parts of the same spacecraft adopt separate potentials; this is known as differential charging. High levels of differential charging can result in electrostatic discharges (ESD), which have been responsible for disruptions in operations, physical damage to surface materials, and even system failures. In 1994, two Telsat telecommunication satellites suffered guidance system failures due to ESD that resulted in service interruptions throughout Canada and an estimated $50-70 million in repair costs and lost revenue [*Leach, 1995*].

The main reason that differential charging occurs on the surfaces of spacecraft is the varying response of the spacecraft's surface materials to the plasma environment. Electrons and ions from the plasma impacting on the spacecraft cause electrons within the surface material to be emitted, which is known as secondary electron (SE) emission. In addition to SE emission, light from the sun stimulates electrons to leave the surface (photo-emission). Secondary and photo-emitted electrons leaving the spacecraft constitute two very important currents from the spacecraft to the plasma. The crucial point is that the amount of photoemission and SE emission depends on the type of material. For example, a shaded metal surface (low SE and photo-emission) near an insulator that is exposed to sunlight (high SE and photo-emission) can lead to high differential charging just due to reduced/enhanced electron emission. Failure to design spacecraft that mitigate this type of charging can result in kilovolt levels of differential charging in certain plasma environments [*Herr, 1994*].

NASA's current plan for protecting spacecraft from harmful differential charging relies heavily on the NASA Charging Analyzer Program (NASCAP), which models surface charging levels in various plasma environments. NASCAP is used by spacecraft engineers to address potential risks due to spacecraft charging.

In order to predict a given surface's current due to SE emission, NASCAP uses a material database based on data from the program's inception in late 1970. Currently, the database is comprised of only 10 materials [*Mandell, 1993*]. Worse yet, many of the parameters for those materials were gathered from literature that predates the technology needed to properly measure SE emission.

The Space Environment and Effects branch of NASA is currently revising NASCAP to address the demands of modern spacecraft design. The research discussed here

involves the measurement of SE emission parameters for a wide range of materials used in spacecraft construction. These measurements will go into the new NASCAP material database and will be the basis for modeling SE emission from spacecraft surfaces, which directly relates to the mitigation of damaging discharge events aboard all future spacecraft.

Secondary Electron Emission

As mentioned, secondary electron (SE) emission is the process of incident (or primary) electrons or ions causing electrons that were originally in the material to be emitted. Since the SE current due to electron bombardment is typically larger than that due to ions, we will only consider SE emission as a result of incident electrons here.

Since an SE and an incident electron that has backscattered are both indistinguishable electrons, the part of the total emitted current that is considered SE emission is defined by energy: SE's are defined by convention as electrons emitted from a material with an energy < 50 eV. An electron emitted with > 50 eV is assumed to be a backscattered electron (BSE) that was originally part of the incident flux. Figure 1 shows a typical energy distribution of all the electrons emitted from a material [*Davies, 1999*]. The arbitrary definition for SE is justified by the fact that the typical SE energy distribution peaks at very low energies (~ 1-5 eV for most materials [*Seiler 1983*]).

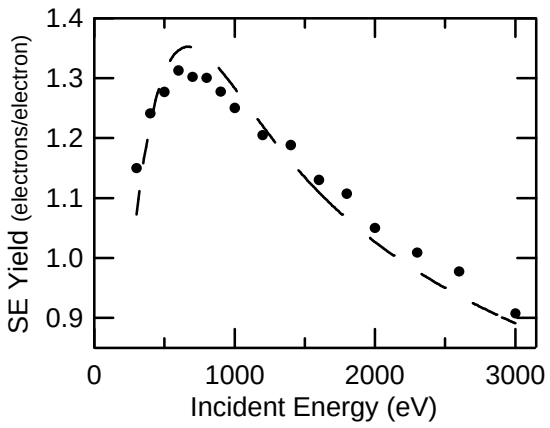

Figure 2. Measured SE yield curve for polycrystalline gold. The dotted line is a three parameter fit with the NASCAP model for SE yield.

The SE parameters that are used in NASCAP describe the number of SE emitted per incident electron of a given energy, or the SE yield $\delta(E)$. Figure 2 shows the NASCAP model's fit to recent measurements by our group of the SE yield curve for polycrystalline gold [*Chang, 2000*]. Given a material's full SE yield curve $\delta(E)$ and the energy distribution of the incident electron flux to a spacecraft surface, NASCAP predicts the SE current from that surface.

In practice, measuring a material's SE yield requires

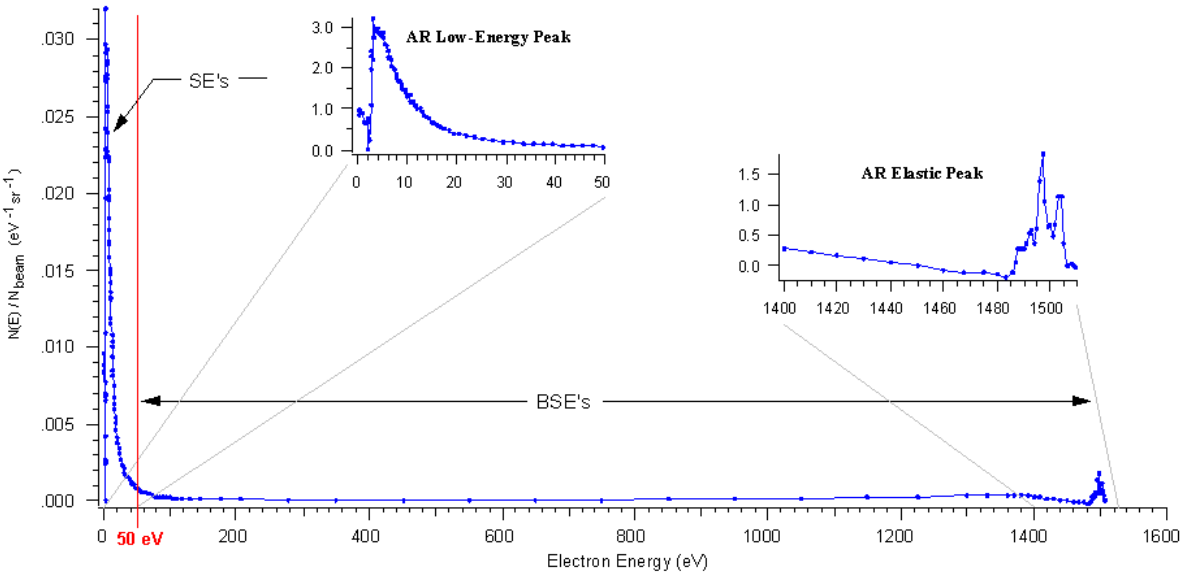

Figure 1. Energy distribution of all electrons emitted from polycrystalline gold due an incident beam of 1.5 keV electrons. The SE and BSE peaks are shown in expanded views. The spectra was taken by a Faraday cup detector (described later) at an angle of 17° with respect to sample normal.

an electron gun to provide a mono-energetic beam of incident electrons, the measurement of the incident beam current I_{beam} and the resulting SE current I_{se} leaving the sample. The SE yield at a given incident beam energy E_{beam} is ratio of those two currents:

$$\delta\left(E_{beam}\right) = \frac{I_{SE}}{I_{beam}} \qquad (1)$$

The design of the apparatus used to measure these currents (hence the SE yield) will be discussed after an overview of the controlled environment in which samples are measured.

Vacuum Chamber

Measuring the SE yield is complicated due to the sensitivity of SE emission to surface contamination. Since SE emission involves the excitation and transport of electrons in a material, the amount of emission depends on the particular electronic environment in a given material. The main factor is the electron's inelastic mean free path (IMFP) in the material, which determines the average length an electron will travel before scattering. Since the IMFP of an electron in a typical material is on the order of nanometers, only a few atomic layers of contamination are necessary to dramatically affect the SE emission properties of a clean material. For example, even a very thin carbon layer on a metal surface will shift the metal's clean SE yield curve to a curve typical of carbon contamination [*Davies, 1997*].

The need for clean, stable surfaces gives rise to the use of ultra-high vacuum (UHV) chambers for the study of SE emission. Figure 3 shows one of the UHV chambers used at Utah State University for SE yield measurements of spacecraft materials. The air in this chamber is pumped out with a mechanical pump (to 10^{-3} torr), then a turbo-molecular pump (to 10^{-7} torr) while being "baked-out" or heated for several days at 150° C to drive out water, and then the chamber is valved off and internally pumped by chemically binding contaminates to liquid-cooled titanium surfaces (to 10^{-10} torr). The final pressure of 10^{-10} torr is defined as UHV, which is equivalent to now having a few particles/cm^3 instead of the nearly 10 trillion particles/cm^3 in atomospheric air. In a UHV chamber there are far fewer contaminates hitting the surface and the sample stays clean for weeks, as opposed to milliseconds in air. Once a sample has been cleaned in UHV by heating or ion sputtering, the SE emission of the clean surface can be measured rather than that of a contaminating oxide or carbon layer.

Sample Stage Design

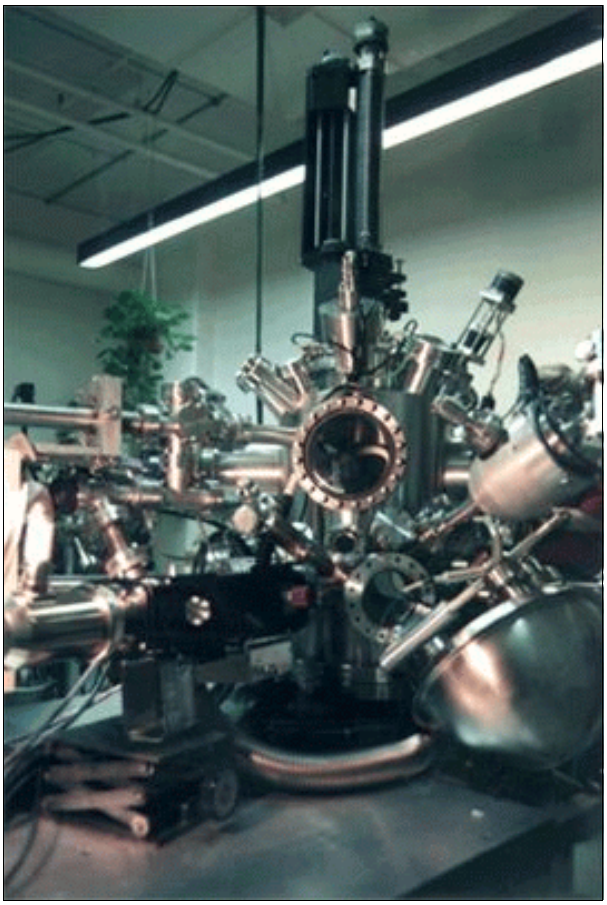

Figure 3. Ultra-high vacuum (UHV) chamber used for SE yield measurements of spacecraft materials.

Working in a UHV chamber also brings unique demands to the design of a holder for the samples inside the chamber (the sample stage) and the SE detector. The most constricting demand is that all the materials must have vapor pressures well below 10^{-10} torr at 150-200° C, otherwise they will outgass while we are baking out the chamber and limit the level of vacuum that can be reached. The list of available materials is effectively limited to Teflon, ceramic, a few specialized polymers, and most metals. For example, metal alloys that contain zinc (e.g. soft solder, some brasses and bronzes, etc.) cannot be used, since zinc has a vapor pressure of 10^{-6} torr at 150° C [*Rosebury, 1965*]. The result of using zinc inside a UHV chamber would be that the "bake-out" portion of pumping down from atmosphere would never reach pressures below 10^{-6} torr.

Another constraint of working in UHV chambers is that access to the sample stage, for wiring or controlling the position, must be gained through the chamber walls via "feed-throughs" that are vacuum tight. The sample

stage is suspended from a rod that can be rotated from the outside and is mounted to several stages of bellows and micrometers that allow for linear motion along three axises, which can be seen on top of the UHV chamber in Figure 3.

In addition to the inherent requirements of the UHV chamber, the sample stage design had to accommodate the particular demands of the purposed SE emission experiments. In specific, the stage needed a design that would:

- Hold multiple samples and allow for easy sample exchange in order to study a large number of materials.
- Enable the measurement of the currents from the sample, stage and electron beam.
- Hold the samples at normal incidence to the beam to avoid accounting for the dependence of the SE yield on the primary electron beam's angle of incidence.
- Use non-magnetic materials near the samples that do not form insulating oxides in order to avoid unwanted electromagnetic fields.
- Use a modular design that gives the flexibility to meet the demands of future research.

The demand for high sample volume was met by a "pie" design with 12 modular pieces, whose faces house samples or various monitoring devices. Figure 4 shows a drawing of the preliminary design. The material for the stage was originally a silicon-bronze alloy; however, availability forced the use of oxygen-free copper (OFHC) even though the material makes small devices difficult to machine. Titanium and molybdenum were also considered, but were immediately abandoned due to the material's expense and extremely difficult machining properties.

Quick sample exchange was originally thought to be satisfied by the use of a UHV gate valve and magnetic transfer arm system; however, the final design allowed for the whole stage to be removed from the chamber via an 8" port. Venting the chamber to atmosphere is avoided by pressuring the chamber briefly with an easily pumped gas, like dry nitrogen. Before removing the stage, 25 wires that carry currents outside via electrical feed-throughs must be unplugged from the stage by means of a UHV compatible, D-type sub-miniature connector (i.e. a printer cable made from an exotic polymer). In practice, the modular nature of the stage and the ability to quickly insert a duplicate stage to avoid exposing the chamber to air were the two demands that made the stage design and fabrication very complicated and time-consuming.

SE Detection Design

The first choice in the design of an SE detector is between the different methods for measuring the SE yield of a material. The incident electron beam current I_{beam} can be measured by directing the beam into a Faraday cup, which is essentially a hole that electrons can enter but not leave. The problem is that the SE current I_{SE} cannot be measured directly. Measuring the current from the sample during electron bombardment is a net current due to I_{beam} and I_{SE} and the backscattered electron current I_{BSE}. Methods for measuring the SE yield rely on the fact that SE's have < 50 eV by definition. There were three methods initially considered for the design of a SE detection device, each with their advantages and drawbacks.

The most common method is to apply a +50 volt bias to the sample, which creates an electric field that returns all the SE's to the sample. The SE current is then given by the difference in the sample current at +50 volts and when grounded. The advantage of this method is the ease of implementation. A standard scanning electron microscope (SEM) is able to take this type of measurement without modification. The main problem is that the electric field between the +50 volt sample and the closest grounded surface (typically the holder) do not necessarily return the SE's to the sample surface.

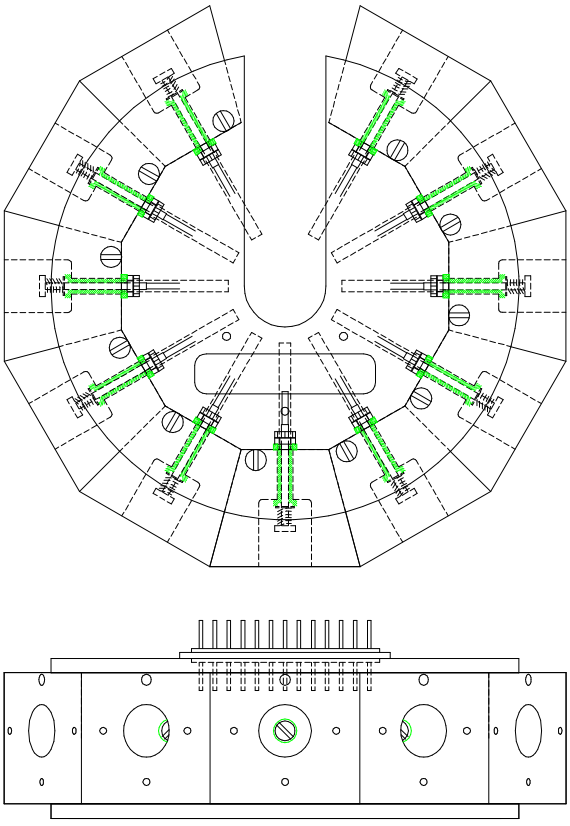

Figure 4. Top and side view of sample stage.

Analysis done by Robert Davies on a similar method estimates the error in the SE yield due to this error can be >20% [*Davies, 1999*]. This method was not pursued in favor of the next two options.

The second method points a Faraday cup at the sample in an effort to measure the SE's emitted from the surface. In contrast to the previous method, a SE are distinguished from a BSE by grounding or applying -50 volts to an aperture inside the Faraday cup, which passes or rejects the SE's. The fact that the Faraday cup only measures a fraction of all the SE's emitted from the sample is overcome by integrating over the theoretical angular distribution of SE's [*Jonker, 1951*]. The disadvantage of this method is the assumption that the emission angle of an SE is maintained until it is detected. Previous work by our group has shown that the angular distribution is distorted by electromagnetic fields that are typical in UHV chambers, even with magnetic shielding [*Nickles, 1999*]. Another disadvantage is that the necessarily small apertures of the Faraday cup result in measuring picoamp (10^{-12} Amp) currents, which is complicated by signal noise. Given these concerns, in comparison to the previous method, this method is feasible and even has some advantages over the method that was finally chosen.

The SE detector was designed after a hemispherical, retarding-grid energy analyzer similar to the apparatus used in low energy electron diffraction (LEED) [*Moore, 1989*]. A cross-sectional drawing of the detector is shown in Figure 6. The sample is surrounded by a hemispherical shell that collects all the electrons emitted from the surface (the collector). In front of the collector is a hemispherical wire grid (bias grid). The bias grid is grounded or biased to -50 volts, which acts to pass or filter out the SE current. The actual details of the SE yield measurement will be discussed later. An inner grid at ground is placed in front of the biasing grid to ensure that the fields created by voltages on the bias grid are relatively anti-parallel to the path of the electrons. A grounded tube allows the incident electron beam to enter through the back of the detector without being affected by potentials on the bias grid or collector.

In contrast to the Faraday cup approach, the hemispherical retarding-grid design does not require integration, the measurement of small currents or the assumption that the SE's maintain their emission angle since the collector covers the whole space around the sample. The main disadvantage comes from electrons scattering off the grid wires that should otherwise be measured by the collector. Errors introduced by the

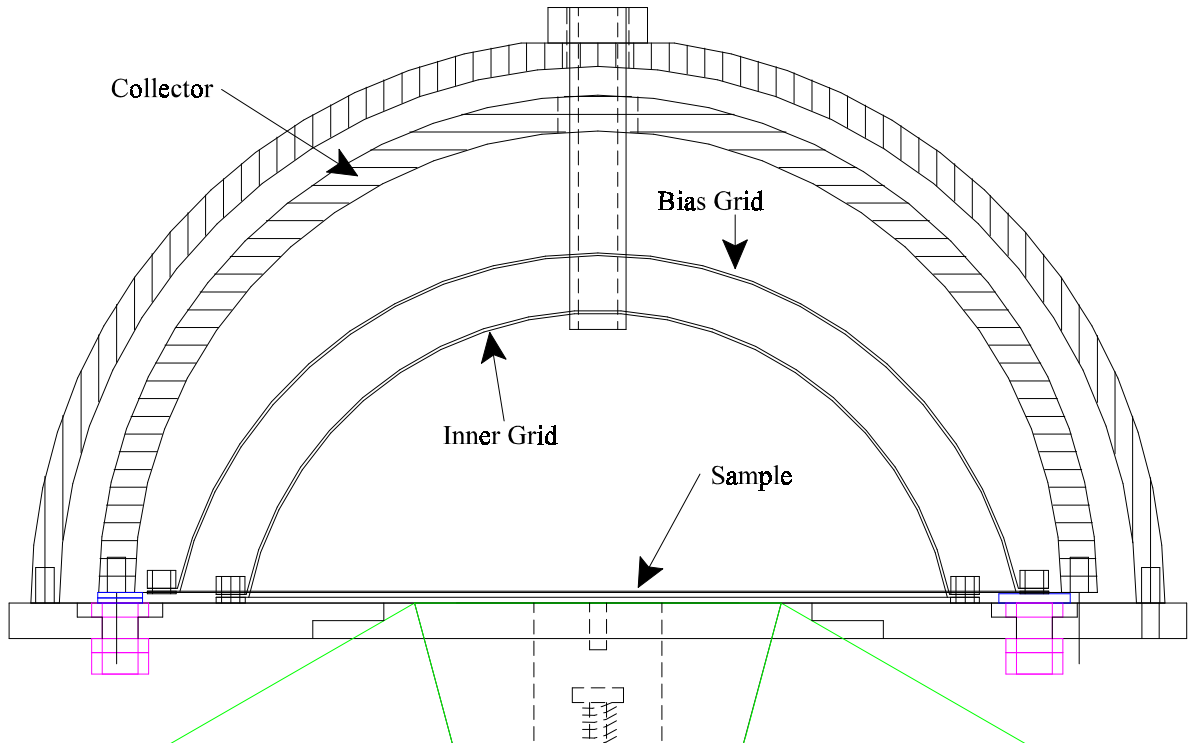

Figure 6. A cross-sectional view (looking down) of the hemispherical grid, retarding-field SE detector.

design were thought to be manageable and will be discussed along with a subsequent review of the measurement technique.

A picture of the completed apparatus is shown in Figure 7. The SE detector is suspended from the same rod that holds the stage to avoid alignment problems. A significant obstacle to the design was the requirement that the detector retain critical sample alignment while being able to move between samples and also move in front of 4 different sources: a 100-2000 eV electron gun, a 3.5-30 keV electron gun, a monochromated UV light source, and a 0.5-5 keV ion gun. Rather than construct four different detectors, the detector is allowed to swivel about the stage axis and is temporarily held in front of a particular sample by pulling a post from the detector against a groove in the stage with a spring. The stage and detector can then rotate as a unit to any of the four sources. Motion between samples is accomplished by rotating the detector up against a fixed rod that overcomes the spring tension and pushes the detector to the groove in front of the next sample.

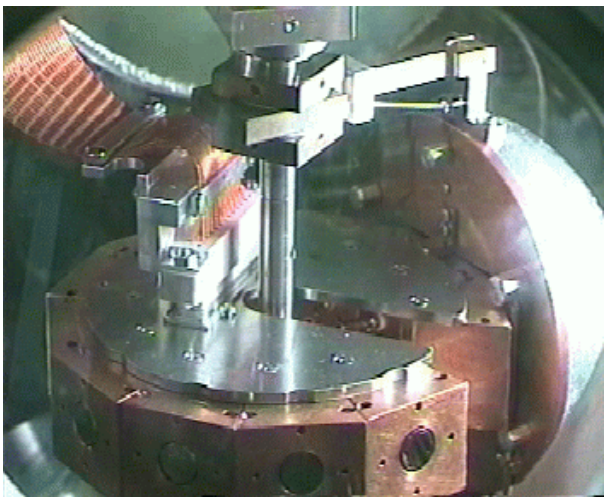

Figure 7. Sample stage and hemispherical SE detector. The cable and connector for the internal wiring can be seen at left.

Measurement of the SE yield

With the hemispherical retarding-grid SE detector, the SE current is measured by taking the difference between the currents measured at the collector in two separate voltage biasing modes:

Collection mode

In this mode the bias grid just before the collector is grounded, which passes all the electrons emitted from the sample. The collector is biased to +50 volts so that all the SE's, created by high energy BSE's impacting the collector, are retained on the collector. Since the bias grid and collector are concentric hemispheres separated by 0.250", the electric fields are strong enough to met this demand. The current measured by the collector is then

$$I_{collector}(+50V) = I_{SE} + I_{BSE} - I_{BSE_C} \quad (2)$$

where I_{BSEc} is the current due to BSE's from the sample also backscattering off the collector.

Suppression Mode

After recording the collection mode current, the bias grid is set to a -50 volt potential and the collector is grounded. The two electric fields between the grounded inner grid, the bias grid at -50 volts, and the collector at ground serve to keep SE's emitted from the sample from passing to the collector and also keep SE's produced on the collector from leaving. The current measured at the collector is then

$$I_{collector}(0V) = I_{BSE} - I_{BSE_C} \quad (3)$$

Notice that the difference between the collector currents in these two modes gives I_{SE}. The SE yield measurement is completed by dividing by the electron beam current I_{beam}, which is measured separately by directing the beam into a specially designed Faraday cup and monitored during the measurement via the current drawn by the electron gun power supply.

As mentioned, the main source of error in the SE yield that is thought to be due to electrons scattering off wires in the two grids that would otherwise be measured during the collection mode. In addition, BSE's from the sample that hit the grid wires will produce SE's that will confound the collector current. In an attempt to reduce these types of error, the grids were made with high open area (84%) wire. In addition, the detector was designed so that the current on the bias grid can be measured. The bias grid current measured during the collection mode is assumed to be an excellent source of information in deriving a systematic correction factor for the SE yield data.

Another small source of error are multiply backscattered electrons returning to the sample and creating SE's, which effectively increases the SE yield. This error was made negligible by coating the inner surfaces of the detector with a colloidal graphite solution and making the detector as large as possible in comparison to the sample. The colloidal graphite has a low BSE yield [*Sternglass, 1953*] and the increased size decreases the chances of returning BSE's hitting the sample.

Conclusions

Preliminary testing of the measurement apparatus and technique has been successful, but refinements are necessary before meaningful results can be presented.

In retrospect, the choice of the hemispherical SE detector method over the Faraday cup was justified. The errors introduced by the hemispherical design are known and manageable, while the Faraday cup inability to collect all the emitted electrons can lead to missing signals and that is hard to overcome experimentally. The design of the sample stage was extremely complicated by the original design goals to hold a large number of samples and quickly exchange stages; however, having made those investments will make data collection proceed quickly.

Acknowledgments

Funding for this research was provided by the NASA Space Environments and Effects Program, the Air Force Office of Scientific Research, and a fellowship from the NASA Rocky Mountain Space Grant Consortium.

References

Chang, W.Y, Dennison, J.R., Kite, J., and Davies, R.E., "Effects of Evolving Surface Contamination on Spacecraft Charging," Proceedings of the AIAA 38th Aerospace Sciences Meeting and Exhibit, Reno NV., 2000.

Davies, R.E., "Evolution of Secondary Electron Emission Characteristics of Spacecraft Surfaces, J. Spacecraft and Rockets, 34, 4, 571-574, 1997.

Davies, R.E., Measurement of angle-resolved secondary electron spectra, PhD Thesis, Utah State University, 1999.

Ford, Kendall, USU Undergraduate Research and Creative Opportunities (URCO) Award, "Development of Improved Faraday Cup for Charged Particle Energy- and Angle-Resolved Cross Sections," April 2000.

Garrett, H.B., "The charging of spacecraft surfaces," Rev. Geophys. Space Phys., 19, 4, 577-616, 1981.

Hastings, D. and Garret, H.B. Spacecraft-Environment Interactions, Cambridge University Press, 1996.

Herr, J.L. and McCollum, "Spacecraft Environments Interactions: Protecting Against the Effects of Spacecraft Charging," NASA Reference Publication 1354, NASA Marshall Space Flight Center, 1994.

James, B.F., coordinator, "The Natural Space Environment: Effects on Spacecraft," NASA Reference Publication 1350, NASA Marshall Flight Center, 1994.

Jonker, J.H.L., "The angular-distribution of the secondary electrons of nickel," Philips Res. Rep., 6, 372-387,1951.

Leach, R.D., "Failures and Anomalies Attributed to Spacecraft Charging," Edited by Alexander, M.B., NASA Reference Publication 1375, NASA Marshall Space Flight Center, 1995.

Vaughan, W.W., Niehuss, K.O., and Alexander, M.B., "Spacecraft Environment Interactions: Solar Activity and Effects on Spacecraft," NASA Reference Publication 1396, NASA Marshall Space Flight Center, 1996.

Mandell M.J., P.R. Stannard, and I. Katz, "NASCAP programmer's reference manual," NASA Lewis Research Center, May 1993.

Moore, J.H., Davis, C.C., and Coplan, M.A., Building Scientific Apparatus, 2nd Ed., Addison-Wesley Publishing, 1989.

Nickles, Neal, R.E Davies, and J.R. Dennison, "Applications of Secondary Electron Energy- and Angular-Distributions to Spacecraft Charging," Proceedings of 6th Spacecraft Charging Technology Conference, Boston, MA., November 1999.

Rosebury, F., Handbook of Electron Tube and Vacuum Techniques, Addison-Weslet Publishing, 1965.

Seiler, H., "Secondary electron emission in scanning electron microscope," J. Appl. Phys.,54,1,R1-R18, 1983.

Sternglass, E.J., An Experimental Investigation of Electron Back-Scattering and Secondary Emission from Solids, PhD Thesis, Cornell University, 1953.

Whipple, E.C., "Potentials of surfaces in space," Rep. Prog. Phys., 44, 1197-1250, 1981.